scientific reports

Check for updates

OPEN

Real-world modeling and simulation for the self-organized toroidal packing of a DNA chain

Satoshi Takatori[1,2]✉, Shusuke Ishida[2,3], Hiroki Okumura[2], Shouichiro Handa[2], Yoichiroh Hosokawa[3], Chwen-Yang Shew[4]✉ & Kenichi Yoshikawa[2]✉

We performed experiments to elucidate the conformations of a single centimeter-sized bead chain through the mechanical vertical agitation under different crowding levels mediated by granular spheres. The bead chain adopted various conformations, such as a compact toroid, swelled toroid, rod-like shape, and random coil, depending on the solution conditions and experimental parameters like the crowding level and strength of the mechanical agitation. The characteristic conformations generated in macroscopic real-world experiments at several tens of centimeters exhibited similarity with those of a single giant double-stranded DNA chain above several tens of kilobase pairs, at several tens of micrometers, despite the significant difference in length scales. We performed Monte Carlo simulation and showed that the conformations of a semiflexible chain captured the essential structural features observed in the bead-chain experiment by adjusting the strength of vertical fluctuation and crowding level, suggesting general features of the semiflexible chain.

Keywords Folding transition of polymer, Crowding effect, Compaction of single polymer chain, Ordered structure caused by fluctuation, Giant DNA, Semiflexible chain

In the field of polymer physics, it has been established that a single flexible polymer chain undergoes a conformational transition from an elongated coil into a compact globule, coil-globule transition, accompanied by a change from a good solvent to a poor solvent[1,2], where the radius of gyration scales as $R_c \sim n^{3/5}$ and $R_g \sim n^{1/3}$, respectively (n is the number of segments and L is the contour length given by $L = nb$, where b is the length of the segment along the direction of the contour line of the polymer chain). The good and bad qualities of the solvent correspond to repulsive and attractive interactions among polymer segments, respectively. Such a universal property of polymer chains indicates that the relative segment density between coil and globule states scales as $\frac{\rho_g}{\rho_c} \sim \frac{R_c^3}{R_g^3} \sim L^{\frac{4}{5}}$, suggesting that the density difference increases with L. In contrast, flexible polymers undergo a continuous coil-globule transition[3–5]. According to extensive experimental studies on single DNA molecule chains[6–12], the transition of individual giant DNA molecules above a size of several tens of kilobase pairs ($\sim 10^4$ base pairs) is discrete, whereas the ensemble average of DNA chains appears continuous as per light-scattering measurements. The discrete nature of the coil–globule transition of a giant DNA molecule is attributed to its semiflexible nature and its property as a polyelectrolyte chain cooperating with counter ions[9,13,14]. Giant DNA molecules exhibit semiflexible characteristics owing to the local rigidity of the double helix structure, with a persistence length (l_p) of approximately 50 nm (approximately 150 bp)[15–17] and a diameter of approximately 2 nm. For such a semiflexible chain, the radius of gyration for coils and globules scales as $R_c \sim \lambda N^{3/5}$ and $R_g \sim (\lambda s N)^{1/3}$, respectively. Here, λ is the Kuhn length ($\lambda = 2\,l_p$), N is the number of Kuhn segments ($N = \frac{L}{\lambda}$), and s is the diameter of a single segment; we assume the dense packing of segments in the globule state. For double-stranded DNA, $\lambda \approx 100$ nm and $s \approx 4$ nm[2]. Based on these relationships, for a DNA chain with $N = 100$ (ca. 30 kbp), the density ratio ($\frac{\rho_g}{\rho_c}$) is assumed to be approximately 10^5. Such a significant difference between coil and compact globules in DNA has been confirmed by measuring individual single DNA molecules using atomic force microscopy (AFM), electron microscopy (EM), and fluorescence microscopy (FM)[6–9,18]. Note

[1]Open Innovation & Collaboration Research Organization, Ritsumeikan University, Ibaragi, Osaka 567-8570, Japan. [2]Faculty of Life and Medical Sciences, Doshisha University, Kyotanabe, Kyoto 610-0394, Japan. [3]Division of Materials Science, Nara Institute of Science and Technology, Ikoma, Nara 630-0192, Japan. [4]Department of Chemistry, College of Staten Island, City University of New York, Staten Island, NY 10314, USA. ✉email: fiddich.2006-12.20@outlook.com; chwenyang.shew@csi.cuny.edu; keyoshik@mail.doshisha.ac.jp

that compact globule DNA molecules show crystal-like regular packing, such as toroids and rods, as shown in Fig. 1. The appearance of these unique morphologies in a semiflexible polymer chain has been examined using numerical simulations[19–23]. From experimental studies, it has been shown that the folding transition of giant DNA molecules into compact globules is generated by the addition of various chemical species such as multivalent cations[7,8], solvable polymers (crowding effect)[6,22,24], and cationic surfactants[25]. The DNA compaction induced by the crowding effect is caused by the depletion effect[6,26–29]. Over the last decade, the crowding effect has attracted considerable interest in relation to the stability and function of various membraneless organelles in living cells[30–34]. Actually, intracellular solutions contain 10–40 wt% biomacromolecules[35,36]. In this study, we investigate the formation mechanism of regular compact structures from a single semiflexible chain under crowding conditions.

Recent studies have focused on understanding the conformation of a chain with coexisting particles[37–44]. Shin et al. performed a 2D computer simulation and found that flexible and semiflexible chains stretched in the presence of active particles for a packing fraction of 0.05, whereas passive particles increased the looping of a chain[39]. Anderson et al. performed a vibrating plate experiment to investigate the effect of active and passive particles on the conformation of a bead chain for an area packing fraction of 0.088[37]. They showed that a granular chain had a high probability of adapting the hairpin structure when mixed with active particles, but the chain coiled in a passive particle bath. A toroidal structure was occasionally observed in a chain immersed in a passive particle bath. We recently conducted an experiment using a fluctuating system containing one or a small number of spherical granular particles coexisting with a large number of smaller particles confined to a cylindrical dish under vertical vibration, as a macroscopic model of polymer chain under crowding conditions. The position of the large spherical particle switched between the boundary and interior of the confined space, depending on the number of small spheres or degree of crowding[38]. We also performed experiments concerning the behavior of a large particle interacting with a large number of small particles confined in dishes with hard/soft boundary conditions under mechanical vibration using a centimeter-scale model[45]. Under a hard boundary condition, the large sphere preferred the boundary at low crowding but tended to localize to the interior under high crowding. Conversely, under a soft boundary condition, the large sphere was localized to the interior under

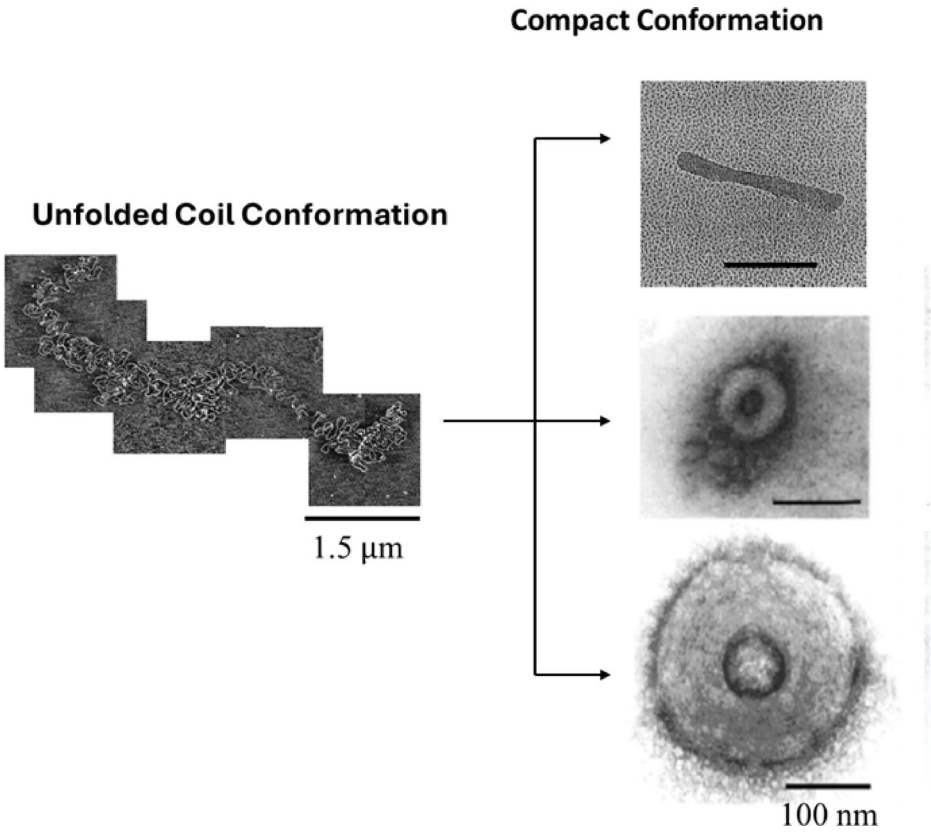

Fig. 1. Morphological variation in DNA. The unfolded conformation is the AFM image of T4 DNA (166 kbp). The compact conformations are the transmission electron microscopy (TEM) images of T4 Gt7 DNA (rod like) and λDNA (toroids). (AFM image reproduced from N. Yoshinaga, K. Yoshikawa, and S. Kidoaki, Multiscaling in a long semiflexible polymer chain in two dimensions, J. Chem. Phys., 116, 9926–9929 (2002) with the permission of AIP Publishing.; TEM images adapted from H. Noguchi, S. Saito, S. Kidoaki and K. Yoshikawa, Self-organized nanostructures constructed with a single polymer chain, Chem. Phys. Lett., 261, 527–533 (1996) with the permission of Elsevier; Y. Yoshikawa, K. Yoshikawa and T. Kanbe, Formation of a Giant Toroid from Long Duplex DNA, Langmuir, 15, 4085–4088 (1999). Copyright 1999 American Chemical Society.)

low crowding and tended to migrate close to the boundary when crowding increased. Note that numerical modeling reproduced essentially the same results for the experimental hard and soft boundary conditions, as a real-world macroscopic model[45,46].

In this work, we performed centimeter-scale macroscopic experimental observations of the behavior of a semiflexible chain. To gain insight into the mechanism of the conformational dynamics of giant DNA molecules exhibiting Brownian fluctuation under crowding conditions, we carried out an experiment for a bead chain coexisting with a large number of microspheres under mechanical vibration/fluctuation and the real-world modeling of a semiflexible polymer chain. The macroscopic real-world modeling showed qualitative similarity of crowding effect for giant DNA molecules for a single semiflexible bead chain at the centimeter scale. In addition, we aimed to develop a numerical simulation model to investigate the dynamic behavior of a semiflexible chain under crowding by referencing the experimental and theoretical studies on genome-sized DNA and the results for a centimeter-sized bead chain.

Experimental materials and methods

We observed the conformational changes in a bead chain inside a cylindrical container under mechanical up–down vibration at different crowding levels by adapting an apparatus (Fig. 2) similar to our previous studies[46,47].

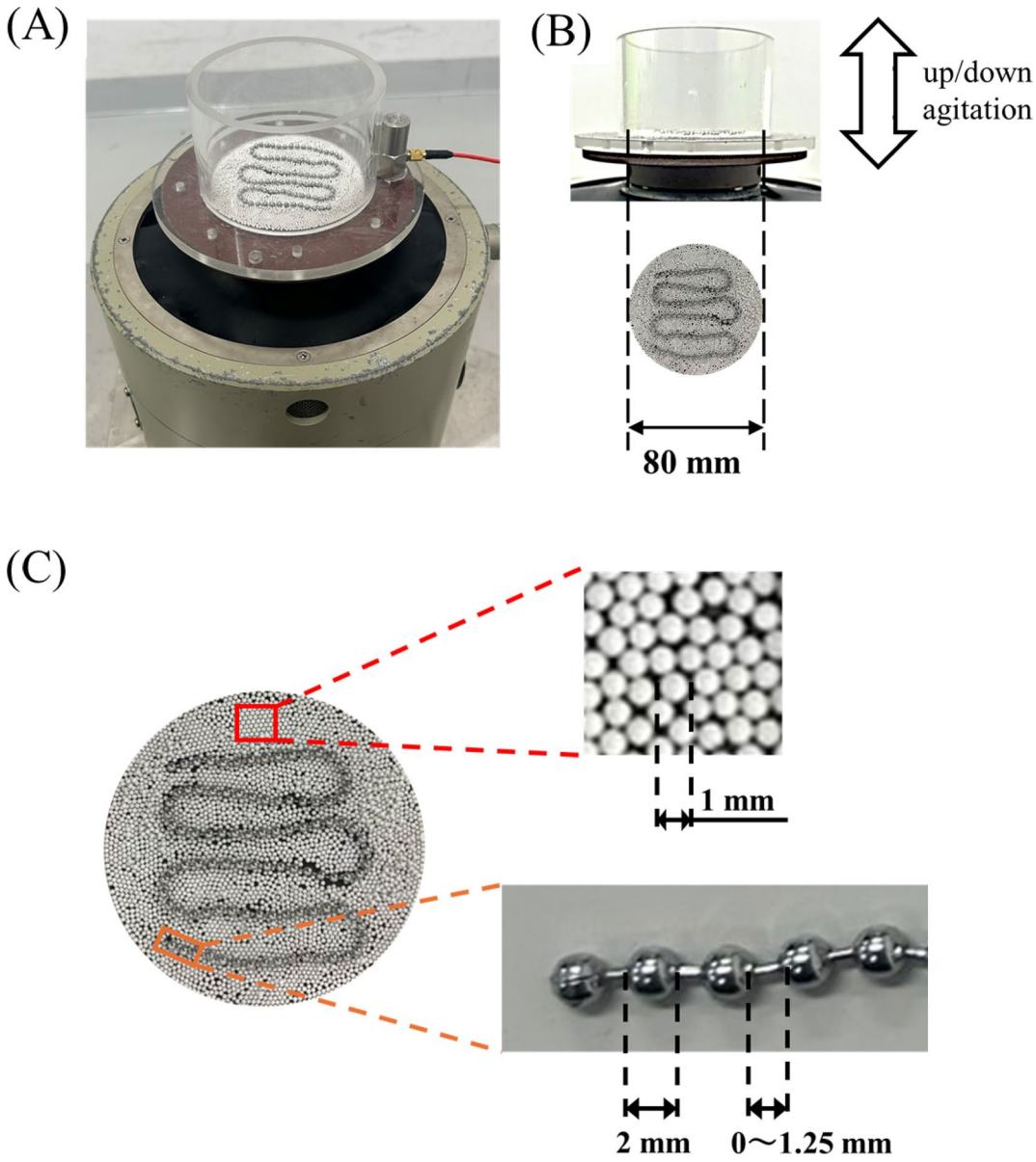

Fig. 2. Experimental system for observing conformational change of a bead chain (contour length: 325 mm) in coexistence with small spherical particles. (**A**) Electromagnetic shaker to apply vertical sinusoidal agitation. (**B**) Side and top views of the cylindrical container. (**C**) Unfolded bead chain with spheres (crowding level of 100%) adapted for the initial condition of the experiments shown in Figs. 3, 4 and 5.

A cylindrical plastic container with an inner diameter of 80 mm was fabricated by the Yoshimoti Factory Company (Osaka, Japan) under a custom order by the authors, and the bead chain was fabricated from 304 stainless steel (Benecreat & Unicraftale). The fully elongated length (contour length) of the bead chain was 325 mm, and the neighboring stainless-steel beads were connected through a narrow rod (2 mm in diameter). The distance between the surfaces of neighboring beads was varied between 0 mm and 1.25 mm almost freely. We mainly performed experiments for the bead chain with a diameter of 2.0 mm and examined the bead chains with diameters of 1.5 mm and 4.0 mm for comparison. We modulated the crowding level by changing the number of spheres in the cylindrical container. The spheres were fabricated from aluminum oxide (93% Al_2O_3 and 5% SiO_2; density: 3.6 g/mL) and had a diameter of 1.0 mm; they were purchased from Nikkato Corporation, Osaka, Japan. We determined the number of spheres such that they occupied the entire inner area of a cylindrical container at a crowding level of 100% in a densely packed state. Vertical vibration was applied using an electromagnetic shaker (512 Series Vibration Generator; EMIC Co., Tokyo, Japan). Sinusoidal agitation [$z(t) = asin(2\pi ft)$] in the vertical direction was applied at a frequency of f = 60 Hz at different amplitudes (a). We adapted the maximum values of acceleration with A = $(2\pi f)^2 a$ = 19.6 m/s^2, 29.4 m/s^2, 39.2 m/s^2, and 49.0 m/s^2, which corresponded to 2 g, 3 g, 4 g, and 5 g, respectively (acceleration due to gravity, g = 9.8 m/s^2). We monitored the time-dependent conformational changes in the bead chain under the mechanical vibration using a digital video camera (EX-100, CASIO Co., Tokyo, Japan) at a frame rate of 30 Hz (Fig. 2).

Results of real-world modeling experiments

Figure 3 shows the time-dependent conformational changes in the bead chain in the container at crowding levels of 25%, 50%, 75%, and 100% under the up–down agitation at the maximum acceleration (A = 2 g) and similar initial confinement, which is indicated by the figures at t = 0 min. The chain shows a partially shrunken conformation at a crowding level of 25% and tends to form a loose-looping conformation at a crowding level of 50% after 10 min. At crowding levels of 75% and 100%, the chain forms swollen and compact toroids, respectively. With respect to the positioning of the chain, loose-looping and swollen chains tend to attach onto the wall of container. On the other hand, the tightly compact toroid positions in the inner region away from the boundary wall. The inside positioning of the compact toroid corresponds well to the theoretical expectation for the specific inner localization of big spherical particle under crowding condition with the confinement of hard boundary condition[45,46]. It is noted that a 100% circular portion with a diameter of less than 20 mm is initially generated (t = 5 min). This circular part pulls the remaining elongated portion over time by forming a tight toroid at 20 min. A similar behavior of the folding transition of a giant DNA chain was captured via single molecular observation in a previous study, which was interpreted in terms of nucleation growth[48]. The differences in the chain conformations depending on the crowding level generated after 20 min vibrational agitation are summarized in Fig. 3B.

Figure 4 shows the time-dependent conformational changes in the bead chain at several accelerations (A = 2 g, 3 g, 4 g, and 5 g) at a crowding level of 100%. The chain becomes less condensed as A increases. At A = 3 g, the chain preferentially shows bundling among segments, in contrast to the compact toroidal conformation at A = 2 g. At A = 4 g and 5 g, the chain adopts an almost unfolded conformation with partial shrinking. The observed conformational changes depending on the strength of the up–down vibration as a measure of A are summarized in Fig. 4B.

We perform experiments by changing the diameter of beads in the bead chain and maintaining a crowding level of 100%, as shown in Fig. 5. Figure 5A shows the time-dependent change in the bead chain with D = 1.5 mm, which is smaller than the chains adapted in the aforementioned experiments (Figs. 2, 3 and 4). The results indicate chain fluctuation with the minimum shrinking at A = 2 g. Similarly, the bead chain with D = 4.0 mm, which is larger than the chains used in the previous experiments, exhibits the minimum shrinkage under A = 2 g. As the vibration strength increases to A = 4 g, the chain tends to form a toroidal conformation with a slightly swollen state.

Framework of numerical modeling

A phenomenological model was developed to capture the essential conformational feature under the steady state in our vibrating plate experiment. First, a single chain with crowders was confined in a cylindrical simulation cell consisting of a rigid bottom and cylindrical boundary, as shown in Fig. 6. The diameter of the cylinder was R_{cyl}. The chain composed of N_m hard spheres with diameter D_m (= σ). Note that σ was also our length unit. The neighboring monomers were connected by a bond, whose length (l_b) randomly varied between σ and 1.8σ by the following potential.

$$\frac{V_{bond}(r_{ij})}{k_BT} = 0 \quad if \quad \sigma \le r_{ij} \le 1.8\,\sigma \\ = \infty \quad otherwise \tag{1}$$

where r_{ij} is the distance between two neighboring monomers, and | i – j | = 1. The bond angle was randomly chosen between θ = 0 and π/4 (where π is radian), resulting in the semiflexible characteristics.

$$\frac{V_{angle}(cos\ \theta_i)}{k_BT} = 0 \quad if \quad 0 \le \theta_i \le \pi/4 \\ = \infty \quad otherwise \tag{2}$$

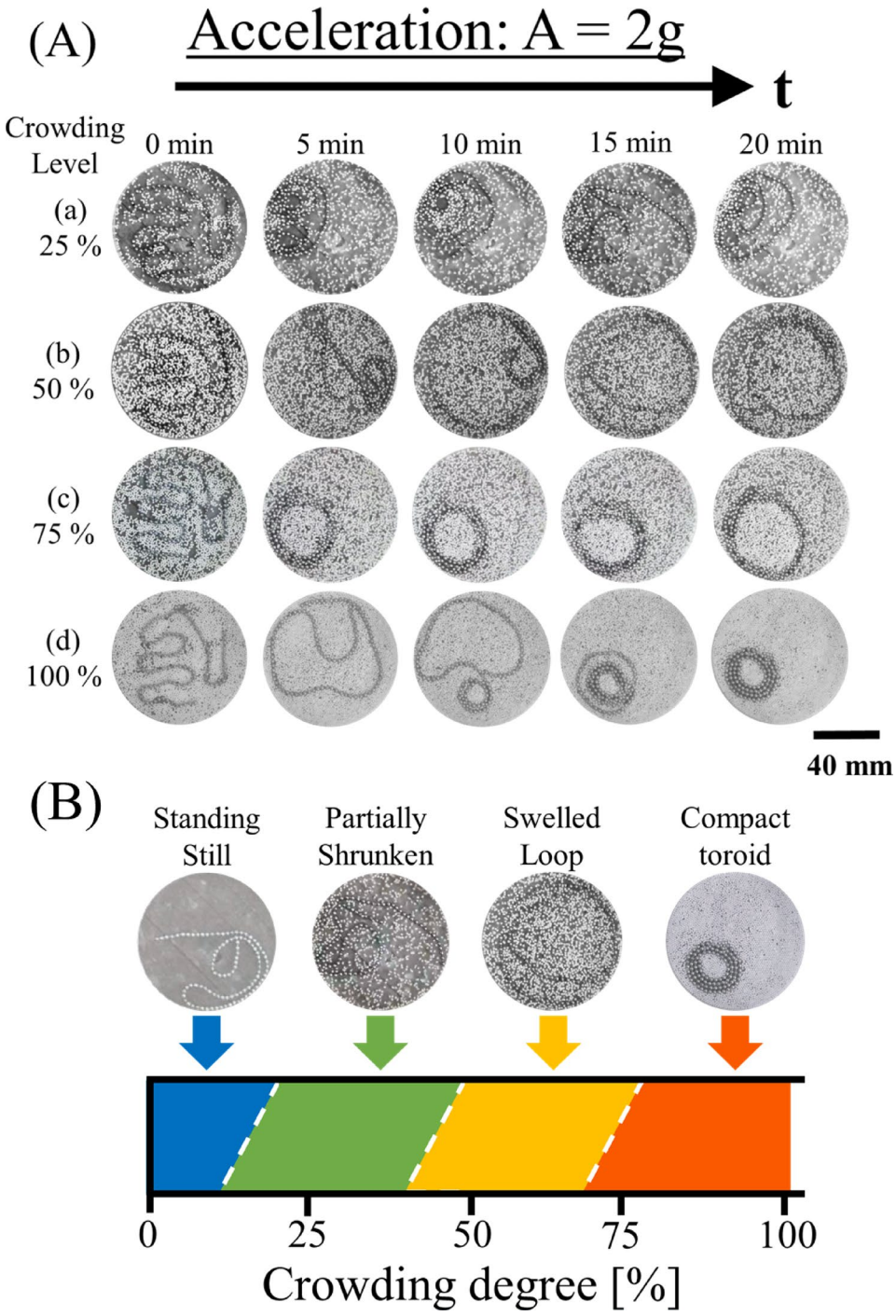

Fig. 3. Effect of different crowding levels on a bead chain in the experimental system shown in Fig. 2. (**A**) Time-dependent changes in the chain conformation under different crowding levels with small spheres (diameter: 1 mm). (**B**) Schematic of the different conformations of the bead chain attained after 15–20 min of vibrational agitation.

where θ_i is the angle between two adjacent bond vectors that join at the i-th monomer, and $1 < i < N_m$. The model resembles the simulation model of a semiflexible chain under confinement in the absence of crowding effect[49].

Like monomers in the chain, crowders were also modeled as rigid spheres of diameter D_c (=0.5σ) and the number of crowders was N_c. The hard core repulsion among different types of rigid particles are given by

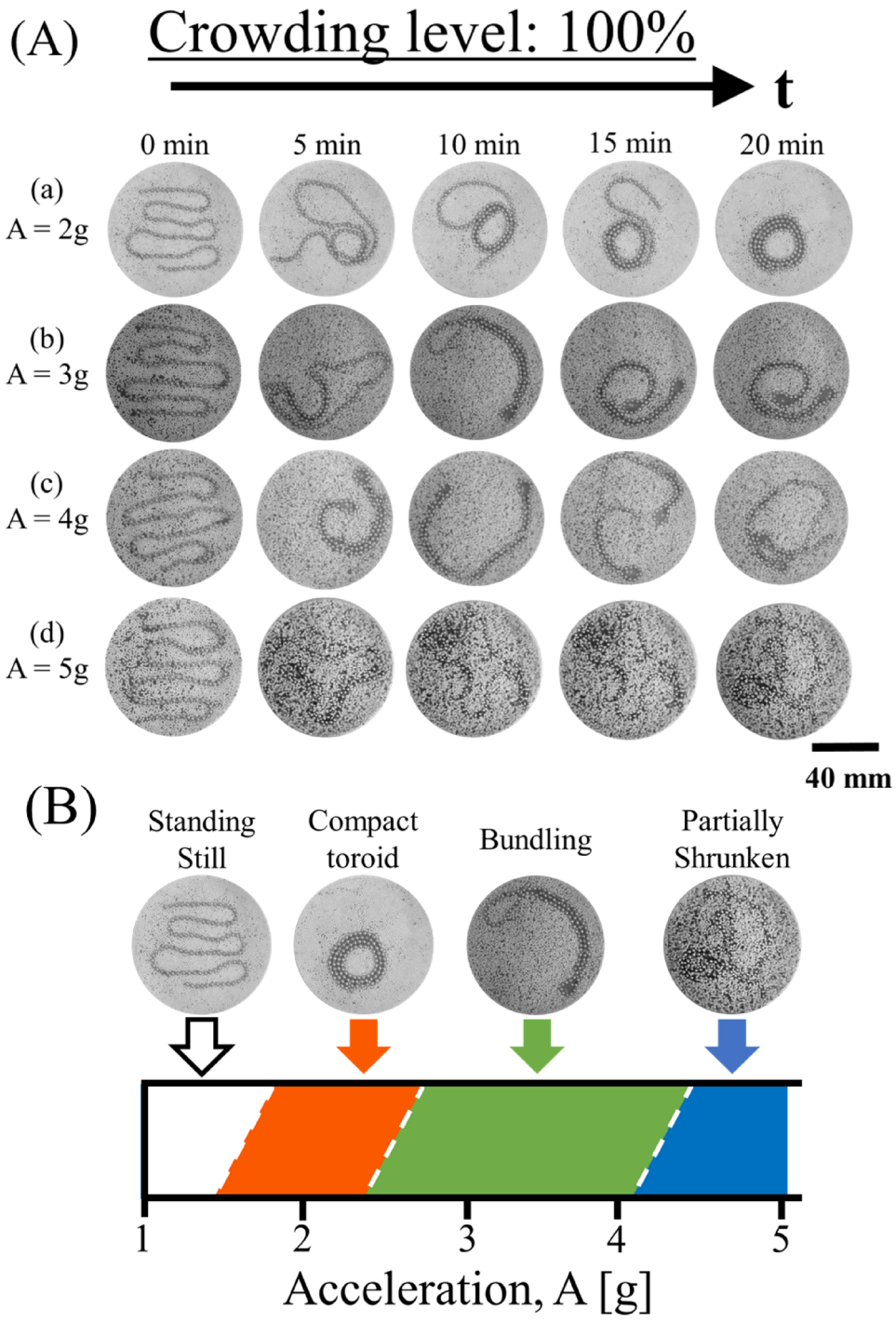

Fig. 4. Effect of magnitude of external vibration on a bead chain under a crowding level of 100% in the experimental system shown in Fig. 2. (**A**) Time-dependent changes in the chain conformation under different vibration amplitudes, represented by maximum acceleration A (g = 9.8 m/s^2). (**B**) Schematic of the different conformations of the bead chain attained after 10–20 min of vibrational agitation.

$$\frac{V_{core}(r_{ij})}{k_B T} = \infty \quad if \quad r_{ij} < \sigma_{ij} \qquad = 0 \quad if \quad r_{ij} \geq \sigma_{ij} \tag{3}$$

where r_{ij} is the distance between the *i*-th and *j*-th particles; k_B is the Boltzmann constant; T is the temperature; $\sigma_{ij} = D_m$, D_s, and $(D_m + D_s)/2$ when both are monomers, both are crowders, and when one is a monomer and the other is a crowder, respectively. Note that the temperature in the experiment can be measured in principle

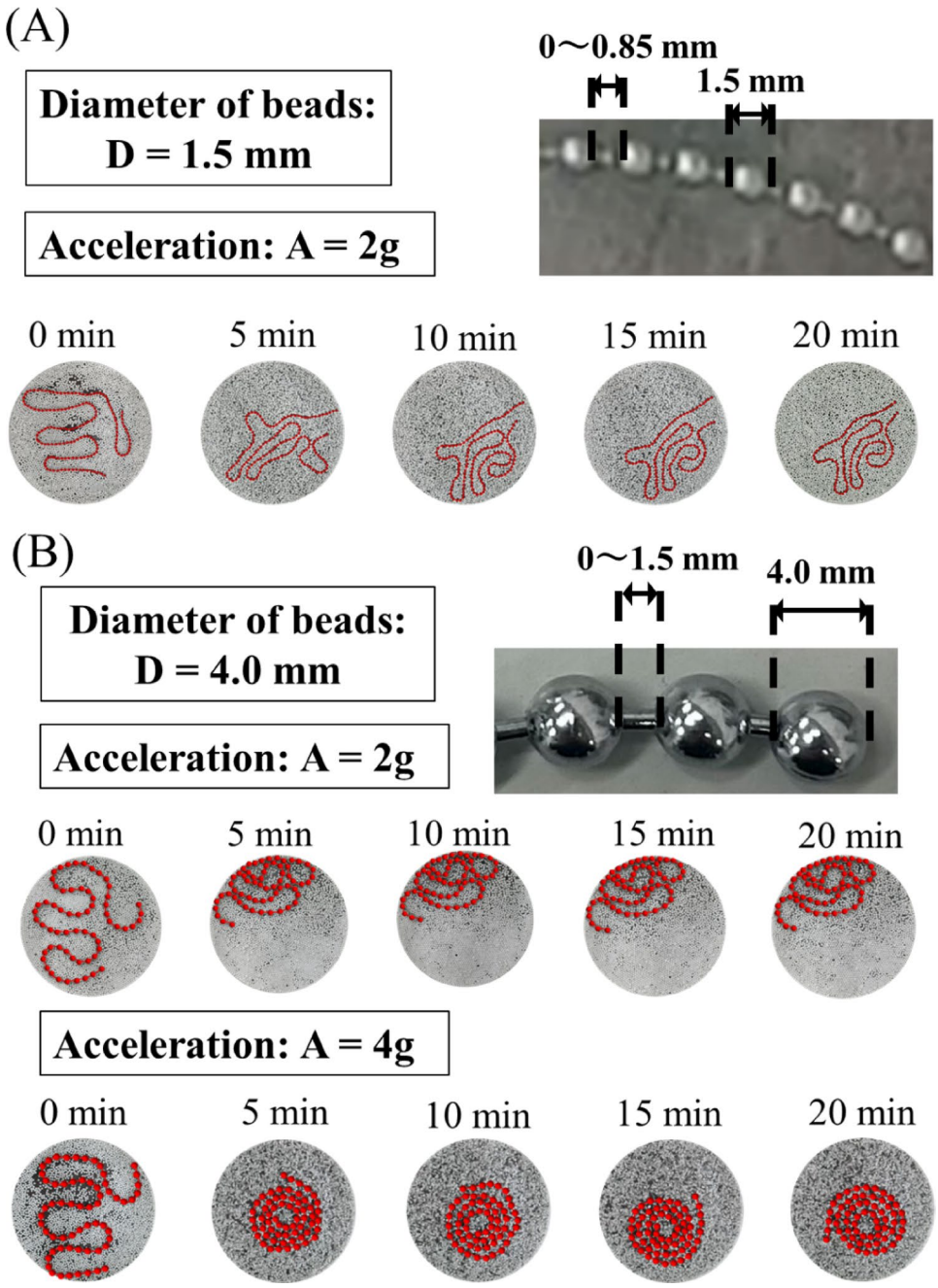

Fig. 5. Effect of small and large diameters of beads (D) in bead chain under a crowding level of 100%. The contour length of the bead chains is ca. 300 mm. (**A**) D = 1.5 mm. (**B**) D = 4.0 mm.

and will be considered in future work. The interaction between a particle and the cylindrical radial boundary is expressed as follows:

$$\begin{aligned} \frac{V_{cyl,r}\,(r_i)}{k_B T} &= \infty \quad if \quad r_i \geq R_{cyl} - D_i/2 \\ &= 0 \quad if \quad r_i < R_{cyl} - D_i/2 \end{aligned} \tag{4}$$

where r_i is the radial distance of the *i*-th particle from the axis of the cylinder, $D_i = D_m$ for a monomer, and $D_i = D_c$ for a crowder. Along the z direction of the simulation cell, particles are subjected to the following potentials as spatial constraints:

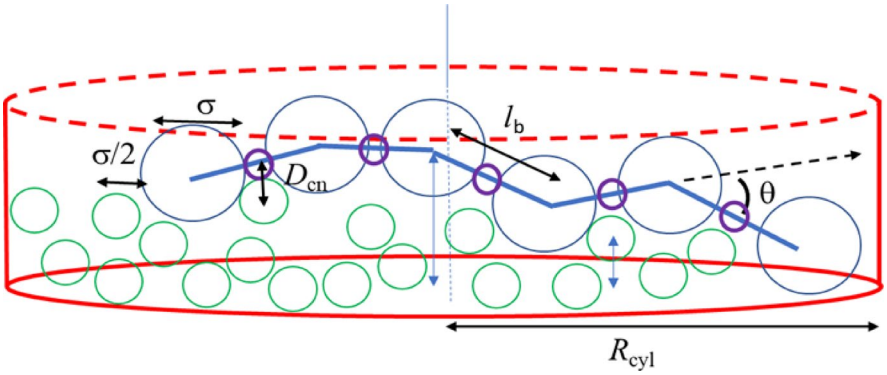

Fig. 6. Schematic of the simulation model consisting of a chain and crowders confined in a cylindrical simulation cell.

Symbols	Physical property	Value or range
σ	Diameter of monomers	
R_{cyl}	Radius of the cylindrical simulation cell	4σ
N_m	Number of monomers of the chain	16
N_c	Number of crowders	230 or 140
D_m	Diameter of spherical monomers	σ
D_c	Diameter of spherical crowders	0.5σ
D_{cn}	Minimum distance between a crowders and connector	$\sqrt{0.2}\sigma$
η_c $(=\frac{N_c D_c^2}{4R_{cyl}^2})$	Packing fraction of crowders	0.90 or 0.55
l_b	Bond length	σ–1.8σ
θ	Bond angle	0–π/4
$h_{m,\,min}$	Maximum vertical height allowed for monomers	0.5σ
$h_{m,\,max}$	Minimum vertical height allowed for monomers	σ or 0.75σ
$h_{c,\,min}$	Maximum vertical height allowed for crowders	0.25σ
$h_{c,\,max}$	Minimum vertical height allowed for crowders	0.75σ

Table 1. Summary of model parameters.

$$\frac{V_{cyl,z}(z_i)}{k_BT} = 0 \quad if \quad H_{i,min} \le z_i \le H_{i,max} \\ = \infty \; otherwise \tag{5}$$

The chain in the experiment had a metal connector to link two neighboring metal beads. A rigid bead of diameter D_{cn} $(=\sqrt{0.2}\,\sigma)$ was inserted between two adjacent monomers to represent the excluded volume of a connector. The connector interacts with other particles as the potential below.

$$\frac{V_{cn}(r_{bi,cj})}{k_BT} = 0 \; if \quad r_{bi,cj} \ge D_{cn} \\ = \infty \; otherwise \tag{6}$$

where $r_{bi,cj}$ is the distance between the i-th connector (connecting i-th and $(i+1)$-th monomers) and j-th crowder and D_{cn} is the minimum distance over which a crowder can reach a connector. Note that a model connector does not interact with monomers. The abovementioned geometric constraints render the chain semiflexible.

To simplify the vertical fluctuation arising from the vibrating plate in the model, the z component was randomly varied between $h_{m,\,mix}$ (= 0.5σ) and $h_{m,\,mix}$ (= σ) for monomers and $h_{c,\,mix}$ (0.25 σ) and $h_{c,\,max}$ (0.75 σ) for crowders. This vertical fluctuation mimicked the tendency for the large monomers to be on top of the crowders due to the Brazil nut effect[50]. The parameters of the model are summarized in Table 1. The above parameters were chosen similar to the experimental condition.

In our previous vibrating plate experiments by mixing a large granular particle with multiple smaller crowders, it was found that the large granular particle was preferentially distributed close to the center of the container for both low and high crowder packing fractions[38,45]. These experiments were unique because all granular particles

were situated in a single layer, which was different from typical bulk granular systems subjected to vertical agitation. Nevertheless, the centralization of the large granular particle on the vibrating plate suggested that smaller crowders might have created a (near horizontal) convection flow towards the center of the plate even in a single-layer system. This inward flow then induced an effective potential to confine monomers towards the center under the steady state. Meanwhile, crowders induced frequently energetic collisions onto the large particle. To combine these effects, a phenomenological potential to depict the interactions between a monomer and a crowder was designed as follow.

$$\frac{V_{flow}\,(x_i, y_i, z_i)}{k_B T} = \Gamma \sum_{j=1}^{N_c} (x_j^2 + y_j^2) \frac{exp(-\kappa\ r_{ij})}{r_{ij}} \tag{7}$$

where (x_i, y_i, z_i) is the position of the *i*-th monomer, Γ is the total strength of the interaction due to coupling of the in-ward flow and particle collisions under vertical agitations, (x_j, y_j) is the horizontal position of the *j*-th crowder on the x–y plane, $1/\kappa$ is the characteristic length of the enhanced collision from a crowder, and r_{ij} is the distance between the *i*-th monomer and *j*-th crowder. A monomer (large particle) was confined to the interior of the vibrating plate by crowders, which is represented by the term $(x_j^2 + y_j^2)$. The energetic collision between a crowder and a monomer caused a stronger repulsive energy that is implemented by an empirical short-range repulsive energy $\frac{exp(-\kappa\ r_{ij})}{r_{ij}}$ with $\kappa\sigma$ set to be 3.5 in the simulation. These two types of interactions were coupled with the strength related to the strength of vertical agitation. Furthermore, it is noted that Γ and κ were not quantitatively derived values but were introduced as effective parameters to mimic the chain behavior observed in the experiment.

Our numerical work was intended to investigate the possibility to correlate the steady state of the highly dissipative vibrating plate experiment with an equilibrium thermodynamics state. As a result, hydrodynamic interactions and white noises were not included. Monte Carlo simulation, without the explicit dynamic information of a system, was a useful tool to sample thermodynamically stable states.

To quantify the crowding level in the simulation, the (area) packing fraction of crowders (η_c) was defined as $\frac{N_c \pi R_c^2}{4R_{cyl}^2}$, which is the fraction of the maximum area coverage from all the particles on the cylindrical simulation cell. Three types of random moves were implemented in the simulation: (1) random walk of monomers, (2) random walk of crowders, and (3) translation of the chain. The step sizes of these motions were selected such that each type of motion has an acceptance ratio of approximately 50%–60%. The equilibrated chain conformation and crowder configuration are insensitive to the step size and proportion of the three types of motions. The total number of steps in the simulation is 1×10^9 – 2.5×10^9.

Results of numerical modeling and comparison with experimental modeling

We first investigated the case when η_c = 0.90, N_m = 16, $h_{m,\,min}$ = 0.5σ, $h_{m,\,max}$ = σ, $h_{c,\,min}$ = 0.5σ, $h_{c,\,max}$ = σ, Γ = 1.2, and κσ = 3.5. Figure 7A shows the temporal evolution of the chain conformation in the Monte Carlo simulation. In the initial configuration, an almost S-shaped chain was placed in the middle of the simulation cell and crowders were aligned in parallel and tightly stacked into two layers in Fig. 7A. In the initial stage, the chain conformation changed from the S shape to the U shape. After the two ends met, one end started to curl inward and exhibited a spiral pattern. A tight toroidal structure was eventually formed at equilibrium. The resulting chirality of the toroid structure was random in the simulation and can be clockwise or counterclockwise in different simulation runs. The two toroid entities shown in Fig. 7A have diameters around 5.8σ (right) and 6.0σ (left), respectively. In this work, all the granular particles interacted through excluded volume interactions. The toroidal conformation observed here can be attributed to the depletion forces caused by the crowding effect, similar to the toroidal chain morphology observed by Anderson et al. from an experiment performed using a bead chain in a bath of passive particles[37]. Nonetheless, our study does not identify the actual pathway for toroid formation in DNA folding. Instead, it is a macroscopic analogy that captures the essential features from geometric and crowding-induced effects.

To test the effect of flow strength, we investigated two cases with the same parameters as those in Fig. 7A except Γ = 2.4 in Fig. 7B and Γ = 0 in Fig. 7C. For Γ = 2.4, the strong flow induced strong compression on the chain, causing a hairpin-like conformation. The loop distributed inward and slightly away from the cylindrical boundary; however, the tail was located next to the boundary. The strong interaction of the monomers with the crowders close to the boundary led to the bending of the tail. A similar conformation was observed by Anderson et al. when a chain was placed in an active particle bath under a strong confinement effect[37].

In the limiting case of Γ = 0, the only interparticle interactions were originated from their excluded volumes. Figure 7C shows that the equilibrium chain conformation exhibited an open ellipse-like structure across the simulation cell. An alternative method for attenuating the effective interaction arising from the granular flow was to reduce the density of crowders. When the packing fraction of crowders is decreased from η = 0.90 to η = 0.55, the chain formed an extremely loose toroid similar to an open circular pearl necklace, as shown in Fig. 7D. Also, the granular chain tended to distribute closer to the boundary, indicating a higher contribution of the depletion force from the crowders (to pin the chain onto the boundary), whereas the effective force of the flow became weakened. In addition, weak monomer–crowder interactions loosened the toroid structure.

Our simulations were carried out with a rather short chain to assure their convergence for the multiple lengthscale system. Nevertheless, Figs. 7A–D show conformations that were similar to the experimental findings. The toroidal structure in Fig. 7 resembled the experimental observation in Fig. 3A at a crowding level of 75% (corresponding to η = 0.75) under A = 2 g and 100% (η = 1.0) with A = 3 g in Fig. 4A. The rod-like structure in Fig. 7B, C with a bent hairpin shape broadly corresponded to the bending conformation in Fig. 4A under

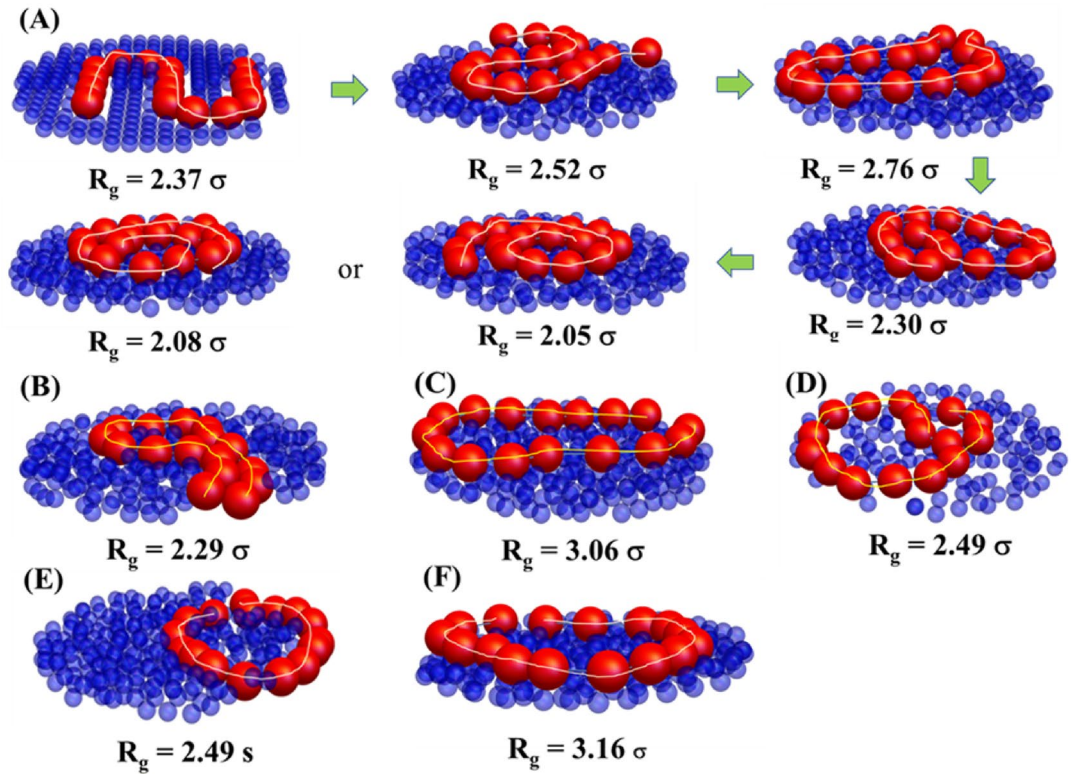

Fig. 7. Schematics of the typical conformational evolution observed during the simulation together with the radius of gyration of chain (R_g) for $\eta_c = 0.90$, $N_m = 16$, $h_{m,\,min} = 0.5\sigma$, $h_{m,\,max} = \sigma$, $h_{c,\,min} = 0.5\sigma$, $h_{c,\,max} = \sigma$, $\Gamma = 1.2$, and $\kappa\sigma = 3.5$ in (**A**). Note that white solid lines trace the chain structure from one end to the other end. Typical chain conformations under the same parameters as those in (a) except $\Gamma = 2.4$ in (**B**), $\Gamma = 0$ in (**C**), and η_c is reduced from 0.90 to 0.55 in (**D**). A typical chain conformation with the same parameters as those in (**A**) except $H_{max,\,m}$ is reduced from σ to 0.75σ in (**E**) and the interaction potential in Eq. (7) is changed to $\frac{V_{flow}(x_i,y_i,z_i)}{k_BT} = \Gamma \sum_{j=1}^{N_c} \frac{exp(-\kappa\ r_{ij})}{r_{ij}}$, without the confinement component in (**F**).

A = 3 g. Furthermore, Fig. 7D shows a loose and wider toroid owing to a lower value of η_c. A similar trend is also observed in Fig. 4A–C, D at a crowding level of 100% under A = 4–5 g. The model developed in this study demonstrated its potential to compare with experimental results in the future. Furthermore, our numerical simulations suggested that the steady state in the vibration experiment may be quantified by a thermodynamic system subjected to an external potential.

In the vibrating plate experiment, vibration caused vertical fluctuation in the granular particles and displayed the Brazil nut effect with larger particles on top of smaller ones. Figure 7E displays a case in which the parameter for the maximum vertical fluctuation of monomers decreases from $H_{max,\,m} = \sigma$ to $H_{max,\,m} = 0.75\sigma$; all other parameters are the same as those shown in Fig. 7. Under this condition, monomers and crowders fluctuated to the same maximum height, that is, $H_{max,\,m} = H_{max,\,c} = 0.75\sigma$. In contrast to the toroid structure observed in Fig. 7A, the chain coiled into an open-ring structure and some part of the ring reached the edge of the boundary. The ring structure originated from different driving forces compared with the loose toroid formation shown in Fig. 7D, in which crowders are mainly underneath the chain. As shown in Fig. 7E, the middle of the ring structure was filled with crowders that hindered chain to further compact into a toroid. In addition, a decrease in $H_{max,\,m}$ led to more significant (horizontal) interactions between crowders and monomers. As a result, the chain is preferentially distributed next to the boundary because the depletion force exerted on the more compact ring structure (as a whole) was significantly enhanced. This indicated the importance of the buoyancy of large monomers in the vibrating plate experiment.

We further investigated the confinement effect induced by the interaction potential in Eq. (7) by transforming the potential into $\frac{V_{flow}(x_i,y_i,z_i)}{k_BT} = \Gamma \sum_{j=1}^{N_c} \frac{exp(-\kappa\ r_{ij})}{r_{ij}}$. In the absence of the confinement component in the potential, the chain coiled in the area close to the cylindrical boundary (Fig. 7F). This chain morphology suggested that strong depletion forces were exerted on individual monomers (a larger diameter) close to the wall. Equation (7) integrated the confinement effect and short-range soft repulsion into one potential function. This expression coincided with our hypothesis that both types of forces were simultaneously present in a granular convection system.

In the present study, we performed numerical investigation under hard boundary condition, being similar to the experimental condition adapted for the granular materials under mechanical vibration. Recently, we have

reported[45,46] that the localization of bigger particles is inverted between hard and soft boundary conditions, as reveled from numerical modeling and macroscopic granular experiments agitated by mechanical vibration. As the extension of the present study, hereafter it would be rather interesting to investigate how the difference of boundary condition causes morphological change for the bead-chain with the coexistence of crowders, through both experimental and numerical studies.

Summary

A simple phenomenological model was devised to elucidate the conformation of a chain mixed with crowders subjected to vertical fluctuation. The model considered the competing pathways for granular convection induced by the vertical vibration of a plate. (1) The flow from the boundary to the center of the plate results in a confinement effect on the chain monomers with a large size. (2) The interaction between a monomer and crowder becomes energetic. (3) The larger monomers tend to be distributed on top of the smaller crowders (Brazil nut effect). The simulation of the model showed that the conformational features of a semiflexible chain were similar to a compact DNA chain above several tens of kilobase pairs and reproduced the essentials in the findings of the vibration plate experiment at the center-meter scale under the crowding level of approximately 50–100% and maximum acceleration of 2–4 g. The consistent conformational morphology among different studies at different length scales suggested the general features of the semiflexible chain.

In this work, the numerical simulations focus on the case of a short chain to test the concepts introduced in the model. The consistent chain conformations observed through the experiment and numerical modeling results indicate that it may be possible to scale the simulation to match realistic experimental conditions. The temperature used in the model can be measured in future experiments by modifying the instruments.

Data availability

Data supporting the findings reported in this manuscript are available from the corresponding authors upon reasonable request.

Received: 9 September 2025; Accepted: 17 November 2025
Published online: 08 December 2025

References

1. Grosberg, A. Y., Khokhlov, A. R. & de Gennes, P. G. *Giant Molecules: Here, there, and Everywhere* 2nd edn (World Sci. Pub. Co., 2010). https://doi.org/10.1142/7199
2. de Gennes, P. G. Collapse of a polymer chain in poor solvents. *J. Phys. Lett.* **36**, 55–57 (1975).
3. Flory, P. J. & Volkenstein, M. Statistical mechanics of chain molecules. *Biopolymers* **8**, 699–700 (1969).
4. de Gennes, P. G. Collapse of a flexible polymer chain II. *J. Phys. Lett.* **39**, 299–301 (1978).
5. Grosberg, A. I., Khokhlov, A. R. & Pande, V. S. *Statistical Physics of Macromolecules* (Springer, 1994).
6. Vasilevskaya, V. V., Khokhlov, A. R., Matsuzawa, Y. & Yoshikawa, K. Collapse of single DNA molecule in poly(ethylene glycol) solutions. *J. Chem. Phys.* **102**, 6595–6602 (1995).
7. Yoshikawa, K., Takahashi, M., Vasilevskaya, V. V. & &Khokhlov, A. R. Large discrete transition in a single DNA molecule appears continuous in the ensemble. *Phys. Rev. Lett.* **76**, 3029–3031 (1996).
8. Shew, C. Y., Higuchi, Y. & Yoshikawa, K. Elucidation of conformational hysteresis on a giant DNA. *J. Chem. Phys.* **127**, 1449131–1449139 (2007).
9. Estévez-Torres, A. & Baigl, D. DNA compaction: fundamentals and applications. *Soft Matter*. **7**, 6746–6756 (2011).
10. Zhou, T., Llizo, A., Wang, C., Xu, G. & Yang, Y. Nanostructure-induced DNA condensation. *Nanoscale* **5**, 8288–8306 (2013).
11. Leforestier, A., Siber, A., Livolant, F. & Podgornik, R. Protein-DNA interactions determine the shapes of DNA toroids condensed in virus capsids. *Biophys. J.* **100**, 2209–2216 (2011).
12. Hud, N. V., Vilfan, I. D. & Toroidal DNA condensates: unraveling the fine structure and the role of nucleation in determining size. *Annu. Rev. Biophys. Biomol. Struct.* **34**, 295–318 (2005).
13. Zinchenko, A. A., Pyshkina, O. A., Lezov, A. V., Sergeyev, V. G. & Yoshikawa, K. Single DNA molecules: Compaction and decompaction. in D*NA Interactions with Polymers and Surfactants* (eds Dias R. & Lindman, B.) Chap. 3, 59–88 (John Wiley & Sons, 2008).
14. Shew, C. Y. & Yoshikawa, K. Elucidation of single molecular observation of a giant DNA. in *Understanding Soft Condensed Matter via Modeling and Computation, Chap. 7* 207–236 (World Scientific, 2010). https://doi.org/10.1142/9789814295598_0008
15. Manning, G. S. The persistence length of DNA is reached from the persistence length of its null isomer through an internal electrostatic stretching force. *Biophys. J.* **91**, 3607–3616 (2006).
16. Yoshinaga, N., Yoshikawa, K. & Kidoaki, S. Multiscaling in a long semiflexible polymer chain in two dimensions. *J. Chem. Phys.* **116**, 9926–9929 (2002).
17. Reisner, W., Pedersen, J. N. & Austin, R. H. DNA confinement in nanochannels: physics and biological applications. *Rep. Prog Phys.* **75**, 1–34 (2012).
18. Zinchenko, A. DNA conformational behavior and compaction in biomimetic systems: toward better Understanding of DNA packaging in cell. *Adv. Colloid Inter Sci.* **232**, 70–79 (2016).
19. Noguchi, H., Saito, S., Kidoaki, S. & Yoshikawa, K. Self-organized nanostructures constructed with a single polymer chain. *Chem. Phys. Lett.* **261**, 527–533 (1996).
20. Noguchi, H. & Yoshikawa, K. First-order phase transition in a stiff polymer chain. *Chem. Phys. Lett.* **278**, 184–188 (1997).
21. Noguchi, H. & Yoshikawa, K. Morphological variation in a collapsed single homopolymer chain. *J. Chem. Phys.* **109**, 5070–5077 (1998).
22. Li, J. et al. Folding transition of single semiflexible polymers controlled by the range of intermonomer attractions. *J. Phys. Chem. B.* **129**, 5343–5353 (2025).
23. Krotova, M. K., Vasilevskaya, V. V., Makita, N., Yoshikawa, K. & Khokhlov, A. R. DNA compaction in a crowded environment with negatively charged proteins. *Phys. Rev. Lett.* **105**, 1283021–1283024 (2010).
24. Mel'nikov, S. M., Sergeyev, V. G., Yoshikawa, K., Takahashi, H. & Hatta, I. Cooperativity or phase transition? Unfolding transition of DNA cationic surfactant complex. *J. Chem. Phys.* **107**, 6917–6924 (1997).
25. Mardoum, W. M., Gorczyca, S. M., Regan, K. E., Wu, T. C. & Robertoson-Anderson, R. M. Crowding induces entropically-driven changes to DNA dynamics that depend on Crowder structure and ionic conditions. *Front. Phys. 6 Article*. **53**, 1–11 (2018).
26. Asakura, S. & Oosawa, F. On interaction between two bodies immersed in a solution of macromolecules. *J. Chem. Phys.* **22**, 1255–1256 (1954).

27. Surve, M., Pryamitsyn, V. & Ganesan, V. Depletion and pair interactions of proteins in polymer solutions. *J. Chem. Phys.* **122**, 1–16 (2005).
28. Groen, J. et al. Associative interactions in crowded solutions of biopolymers counteract depletion effects. *J. Am. Chem. Soc.* **137**, 13041–13048 (2015).
29. Gupta, A. N. & Van der Maarel, J. R. C. Compaction of plasmid DNA by macromolecular crowding. *Macromolecules* **50**, 1666–1671 (2017).
30. Uversky, V. N. Intrinsically disordered proteins in overcrowded milieu: Membrane-less organelles, phase separation, and intrinsic disorder. *Curr. Opin. Struct. Biol.* **44**, 18–30 (2017).
31. André, A. A. M. & Spruijt, E. Liquid–liquid phase separation in crowded environments. *Inter J. Mol. Sci.* **21**, 5908 1–20 (2020).
32. Monterroso, B. et al. Macromolecular crowding, phase separation, and homeostasis in the orchestration of bacterial cellular functions. *Chem. Rev.* **124**, 1899–1949 (2024).
33. Musacchio, A. On the role of phase separation in the biogenesis of membraneless compartments. *EMBO J.* **41**, e109952/1–20 (2022).
34. Rivas, G. & Minton, A. P. Macromolecular crowding in vitro, in vivo, and in between. *Trends Biochem. Sci.* **41**, 970–981 (2016).
35. Zimmerman, S. B. & Trach, S. O. Estimation of macromolecule concentrations and excluded volume effects for the cytoplasm of Escherichia coli. *J. Mol. Biol.* **222**, 599–620 (1991).
36. Kuznetsova, I. M., Turoverov, K. K. & Uversky, V. N. What macromolecular crowding can do to a protein. *Inter J. Mol. Sci.* **15**, 23090–23140 (2014).
37. Anderson, C. J., Briand, G. & Dauchot, O. Fernández-Nieves, A. Polymer-chain configurations in active and passive baths. *Phys. Rev. E*. **106**, 064606 (2022).
38. Oda, S., Kubo, Y., Shew, C. Y. & Yoshikawa, K. Fluctuations induced transition of localization of granular objects caused by degrees of crowding. *Phys. D*. **336**, 39–46 (2016).
39. Shin, J., Cherstvy, A. G., Kim, W. K. & Metzler, R. Facilitation of polymer looping and giant polymer diffusivity in crowded solutions of active particles. *New. J. Phys.* **17**, 1–12 (2015).
40. Knight, J. B. et al. Experimental study of granular convection. *Phys. Rev. E*. **54**, 5726–5738 (1996).
41. Harder, J., Valeriani, C. & Cacciuto, A. Activity-induced collapse and Reexpansion of rigid polymers. *Phys. Rev. E*. **90**, 1–4 (2014).
42. Shew, C. Y. & Yoshikawa, K. A toy model for nucleus-sized crowding confinement. *J. Phys. Cond Matt*. **27**, 0641181–0641187 (2015).
43. Gu, L. et al. Complex phase transition of DNA condensation under crowding confinement conditions. *Phys. A*. **507**, 489–498 (2018).
44. Chauhan, G., Simpson, M. L. & Abel, S. M. Adsorption of semiflexible polymers in crowded environment. *J. Chem. Phys.* **155**, 0349041–0349049 (2021).
45. Kuroda, M., Takatori, S., Kenmotsu, T., Yoshikawa, K. & Shew, C. Y. Stiffness of confinement controls the localization of an object under crowding: macroscale real-world and microscale numerical modelings on the specificity of intracellular positioning. *J. Phys. Soc. Jpn*. **92**, 1–9 (2023).
46. Shew, C. Y., Oda, S. & Yoshikawa, K. Localization switching of a large object in a crowded cavity: A rigid/soft object prefers surface/inner positioning. *J. Chem. Phys.* **147**, 2049011–2049011 (2017).
47. Takatori, S., Baba, H., Ichino, T., Shew, C. Y. & Yoshikawa, K. Cooperative standing-horizontal-standing reentrant transition for numerous solid particles under external vibration. *Sci. Rep.* **8**, 1–11 (2018).
48. Yoshikawa, K. & Matsuzawa, Y. Nucleation and growth in single DNA molecules. *J. Am. Chem. Soc.* **118**, 929–930 (1996).
49. Fosnaric, M., Iglic, A., Kroll, D. M. & May, S. Monte Carlo simulations of a polymer confined within a fluid vesicle. *Soft Matter*. **9**, 3976–3984 (2013).
50. Rosato, A., Strandburg, K. J., Prinz, F. & Swendsen, R. H. Why the Brazil nuts are on top: size segregation of particulate matter by shaking. *Phys. Rev. Lett.* **58**, 1038–1040 (1987).

Acknowledgements

We thank Prof. Takashi Kenmotsu for the useful advice concerning the mechanism of folding transition of semiflexible chain. CYS thanks the support from the PSC-CUNY awards.

Author contributions

S.T., S.I., Y. H., C.-Y. S., and K. Y. conceived this research project. S.T., S.I., H.O. and S.H. performed the experiments. C.-Y. S. performed numerical simulations. S.T., S.I., C.-Y.S. and K.Y. wrote the paper.

Funding

C.-Y. S. was funded for theoretical modeling of this research by the PSC-CUNY award # 67125-00 55, administered by the Research Foundation of the City University New York (RF-CUNY).

Declarations

Competing interests

The authors declare no competing interests.

Additional information

Correspondence and requests for materials should be addressed to S.T., C.-Y.S. or K.Y.